frontiers in Materials

ORIGINAL RESEARCH
published: 17 August 2021
doi: 10.3389/fmats.2021.719563

Occurrence State of Carbon and Electrolyte in Anode Carbon Residue From Electrolytic Aluminum

Song Mao[1,2,3] *and Qin Zhang*[2,3,4]*

[1]College of Resources and Environmental Engineering, Guizhou University, Guiyang, China, [2]National and Local Joint Laboratory of Engineering for Effective Utilization of Regional Mineral Resources from Karst Areas, Guiyang, China, [3]Guizhou Key Laboratory of Comprehensive Utilization of Non-metallic Mineral Resources, Guiyang, China, [4]Guizhou Academy of Science, Guiyang, China

Anode carbon residue is produced in the production of electrolytic aluminum. Its properties need to be studied for secondary utilization. In this paper, mineralogy of anode carbon residue from an electrolytic aluminum plant in Guizhou was studied. The anode residue chemical composition, structure, mineral composition, occurrence state of main elements, etc, was investigated. The results show that: Anode carbon residue is mainly composed of 14 minerals such as cryolite, cryolithionite, elpasolite and graphite. Among them, the opaque minerals are mainly graphite and the transparent minerals are mainly cryolite. Carbon in the form of independent mineral occurrence in graphite; fluoride in the form of independent mineral occurrence in cryolite, cryolithionite, elpasolite and fluorite; aluminum in the form of independent mineral occurrence in cryolite, cryolithionite, elpasolite, aluminium oxide and magnesium aluminate; sodium in the form of independent mineral occurrence in cryolite, cryolithionite, elpasolite. The mineralogical characteristics and occurrence state of carbon and electrolyte were studied, which provided a basis for the separation and recovery of carbon and electrolyte in anode carbon residue.

Keywords: anode carbon residue, mineral composition, state of occurrence, graphite, cryolite

OPEN ACCESS

Edited by:
Lijie Guo,
Beijing General Research Institute of Mining and Metallurgy, China

Reviewed by:
Huamei Duan,
Chongqing University, China
Jiaqi Li,
University of California, United States

***Correspondence:**
Qin Zhang
zq6736@163.com

Specialty section:
This article was submitted to Structural Materials, a section of the journal Frontiers in Materials

Received: *03 June 2021*
Accepted: *28 June 2021*
Published: *17 August 2021*

Citation:
Mao S and Zhang Q (2021) Occurrence State of Carbon and Electrolyte in Anode Carbon Residue From Electrolytic Aluminum. Front. Mater. 8:719563. doi: 10.3389/fmats.2021.719563

INTRODUCTION

Hall-Heroult electrolysis process is the most commonly used method for aluminum production (Grjotheim and Krohn, 2020). Anode carbon residue produced in the process of electrolytic aluminum is a kind of dangerous solid waste. For example, it contains fluorine ions, the direct storage and landfill treatment will have a serious impact on the environment (Lifeng et al., 2019). Carbon anode is one of the key components in the production of electrolytic aluminum. It is mainly composed of calcined petroleum coke, coal tar pitch and regenerated carbon materials (Bhattacharyay et al., 2017). In the process of electrolytic aluminum production, part of the carbon anode falls off and enters the electrolyte to form anode carbon residue, and the accumulation of carbon residue will affect the production of electrolytic aluminum (Jin-sheng and Qing-chun, 2017; Zhi-qian et al., 2019), and the generation of carbon residue is related to the quality of anode (Aryanpour et al., 2014; Chevarin et al., 2015). Because in the process of aluminum electrolysis, carbon anode participated in the electrolysis process and was consumed, the production of aluminum at the same time to consume a large amount of carbon, producing a large amounts of CO_2 (Huang et al., 2018) are produced resulting in voltage increases (Haupin, 1971) and current efficiency losses (Einarsrud, 2010). The carbon anode needs to be replaced in time after being consumed, to ensure the normal operation of production (Chevarin et al., 2015; Allard et al., 2019; Guo et al., 2020; Hussein et al., 2020). The production of anode carbon residue can be reduced

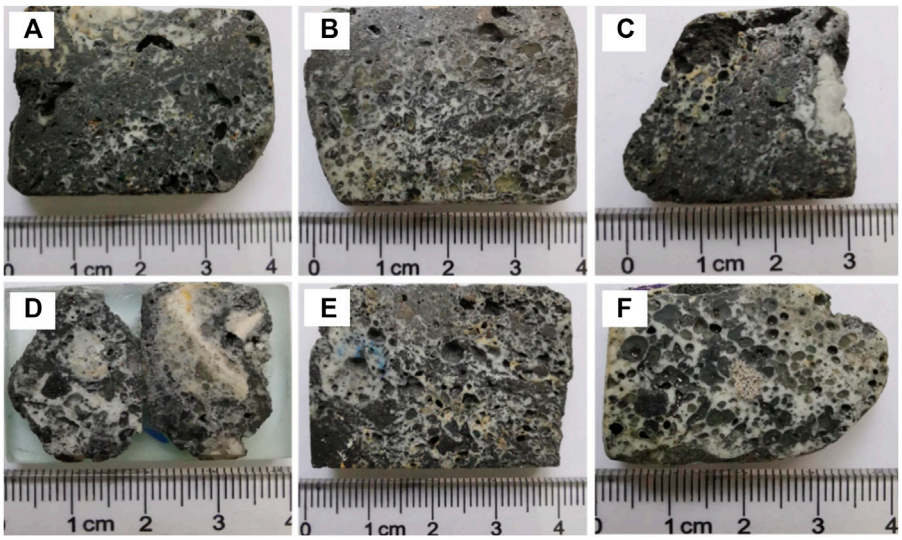

FIGURE 1 | Structure Diagram of Anode Carbon Residue. **(A–D)** Many pores, cryolite and graphite are locally enriched; **(E,F)** Multiple pores, alternating distribution of cryolite and graphite.

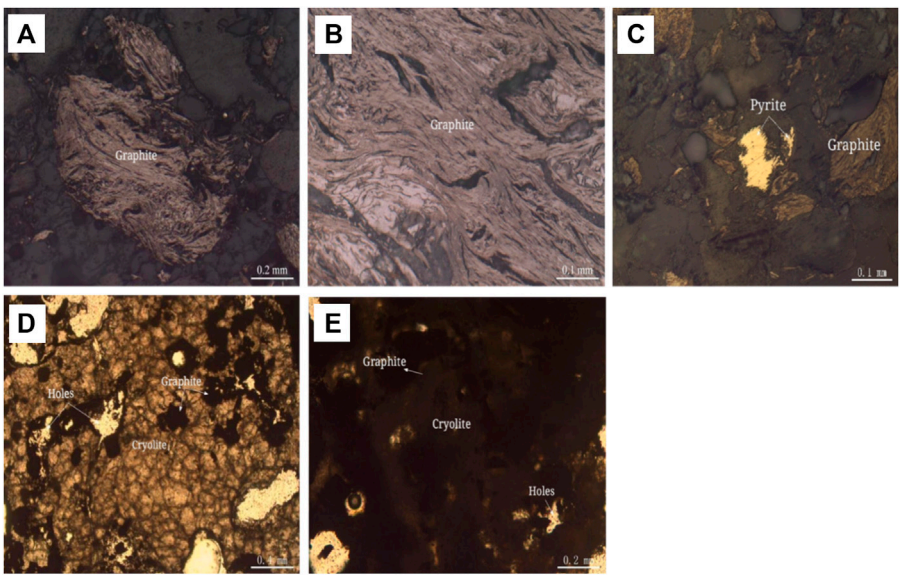

FIGURE 2 | Structure Diagram of Anode Carbon residue. **(A)** Flake and fibrous graphite aggregates are lumpy in reflected plane polarized light. **(B)** Flake and fibrous graphite is lumpy in reflected plane polarized light. **(C)** Pyrite is anamorphic granular in reflected plane polarized light. **(D)** Cryolite is microscopic granular amorphous, grain boundaries are blurred, closely inlaid, graphite aggregates embedded in them, transmission of single polarized light. **(E)** cryolite is mud-microcrystalline, particle size <0.004 mm, or 0.004–0.03 mm, transmission of single polarized light.

TABLE 1 | Chemical multi-element analysis results/%.

Chemical element	**F**	**Al**	**Na**	**K**	**S**	**Ca**	**Mg**
Content	43.27	11.77	22.44	2.77	0.42	1.58	0.39
Chemical element	**Si**	**Fe**	**C_{total}**	**$C_{organic}$**	**Ni**	**LOI 700 °C**	**LOI 1,000 °C**
Content	<0.50	0.58	14.16	12.28	0.23	16.53	31.00

"LOI" means loss on ignition in bold.

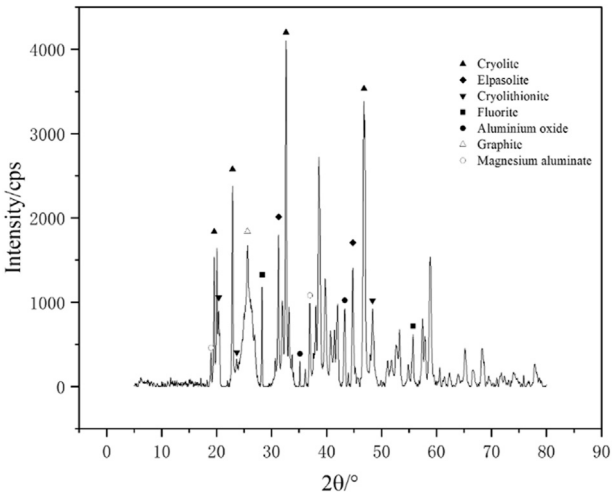

FIGURE 3 | X-ray diffraction analysis results of anode carbon residue.

by improving the quality of raw materials and strengthening the management of electrolytic aluminum production process (Haifei et al., 2009; Qing et al., 2015). It has been found that the shape of anode is one of the factors affecting the formation of carbon slag (Min-zhang and Xian, 2012). The anode consumption can be reduced by optimizing the structure of anode carbon block height and top shape (Xugui, 2021). The anode performance can also be improved by increasing the density of carbon anode, reducing the resistivity, air permeability, and reducing the impurity elements in the anode carbon (Batista and da Silveira, 2008; Dan-qing, 2008; Azari et al., 2013; Azari et al., 2013; Khaji and Al Qassemi, 2016). Trace elements in anode will affect anode consumption and aluminum liquid quality (Jing et al., 2010; Jing-lu et al., 2015). At the same time, the carbon and electrolyte in the anode carbon residue can be separated and recovered, which can effectively utilize the solid waste resources (Xiangyang et al., 2016; Lifeng et al., 2019). In the study of alternative materials for carbon anode, some researchers use calcined anthracite to partially replace petroleum coke to produce carbon anode (Yao-jian et al., 2009), and some researchers use bio-asphalt instead of coal asphalt to prepare carbon anode (Hussein et al., 2020). The use of inert materials instead of carbon anodes will be a promising option for the future and has been extensively investigated (Xiao et al., 2014; Kubiňáková et al., 2018). In view of the current utilization of anode carbon residue, the recycling of anode carbon residue is one of the effective ways to solve the environmental problems caused by it. The separation and recovery of carbon and electrolyte and the quantification of the key mineralogical parameters in anode carbon residue are important means for the separation of useful components (Diógenes et al., 2021).

In this paper, Polarized light microscope and X—ray diffraction (XRD), Scanning Electron Microscope and Energy Dispersive Spectroscopy (SEM-EDS) Analysis and combined with mineral liberation analyser (MLA), and other methods for anode carbon residue was studied, find out the structure of the anode residue structure, element composition, mineral composition and embedded characteristics, find out the carbon phase, sodium, aluminum phase, fluorine equal characteristics of each phase found out C, F, Al, Na, K and other elements in the distribution law of various minerals and occurrence state, It provides a basis for the separation and recovery of useful components in anode carbon residue.

MATERIALS AND METHODS

Anode carbon residue is taken from Guizhou Hua Ren New Material Co., Ltd. The bulk anode carbon residue was selected and polished, and the structure of the anode carbon residue was analyzed by polarizing microscope (Axio Scope. A1, Zeiss, Germany), chemical multi-element analysis, X-ray diffraction analysis (Empyrean sharp shadow, Panalytical, Netherlands), MLA mineral dissociation analyzer (MLA650, FEI, American), scanning electron microscopy (Quanta600, FEI, American) and energy dispersive X-ray spectrometry (Apollo X type, EDAX, American) were used to analyze the element composition, mineral composition, embedded characteristics, symbiosis and element occurrence of anode carbon residue.

TEST RESULTS AND DISCUSSION

Structure of Anode Carbon Residue

The gross eye observation shows that the anode carbon residue is black, and the particle size less than 5 cm. In some anode carbon residue, dark mineral aggregates and light mineral aggregates are locally enriched, with multiple pores and porous structures. The structural diagram is shown in **Figures 1A–D**. Dark mineral aggregates and light mineral aggregates are alternately distributed, and the structural diagram is shown in **Figures 1E, F**.

Polarizing microscope was used to analyze the anode carbon residue. The opaque minerals in the anode carbon residue were mainly graphite, which was flaky and fibrous, forming flaky and fibrous crystalloblastic structures. Transparent minerals are mainly cryolite, cryolithionite and elpasolite, which are microscopic granular, mud-microcrystalline, forming micro-granular metamorphosis structure and mud-microcrystalline structure. The metallic minerals are mainly pyrite, magnetite, polydymite and pentlandite, which are anisotropic granular and constitute anisotropic granular structure.

Flake and fibrous crystallizing structure: graphite in anode carbon residue has good crystallizing degree, showing flaky and fibrous shape; aggregates are twisted into lumps, camboidal polygonal and other amorphous particles, which are distributed in anode carbon residue, as shown in **Figures 2A, B**. Anisotropic granular structure: there are very few metallic minerals in the anode carbon residue, which are mainly pyrite, magnetite, polydymite and pentlandite. The anisotropic granular structure is formed, as shown in **Figure 2C**. Micro-granular crystalloblastic structure: the main transparent mineral cryolite in anode carbon residue is semi-idiomorphic and other-shaped granular with particle size <0.1 mm. The particles are closely

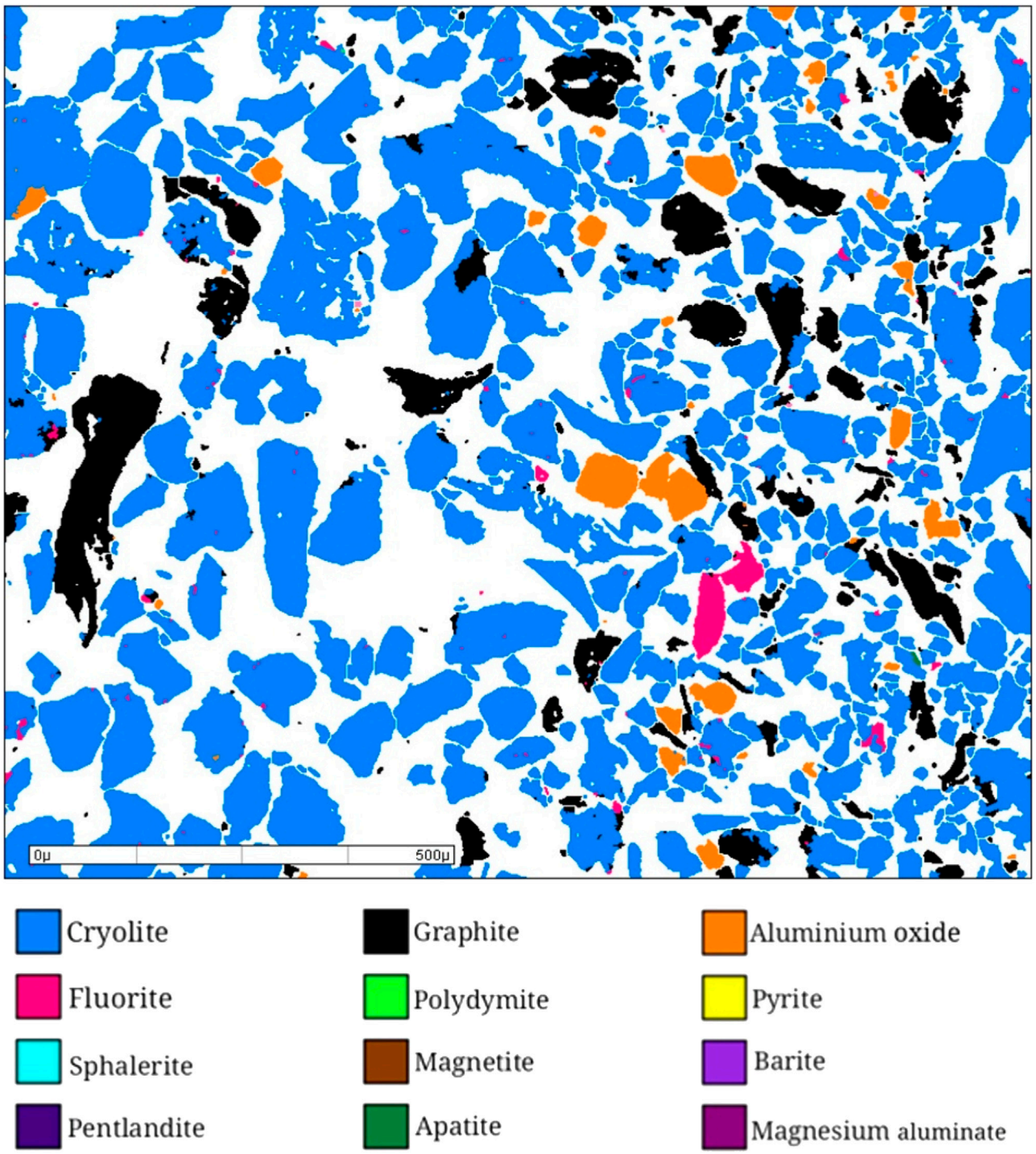

FIGURE 4 | General diagram of MLA analysis of anode carbon redidue (partial area).

inlaid to form a micro-granular crystalloblastic structure, as shown in **Figure 2D**. Mud-microcrystalline structure: part of cryolite in anode carbon residue has fine crystalline particle size, showing micrite size <0.004 mm, or micrite size between 0.004 and 0.03 mm, forming mud-microcrystalline structure, as shown in **Figure 2E**.

TABLE 2 | Mineral composition and content table/%.

Serial	Mineral name	Chemical formula	Content (%)
1	Cryolite	Na_3AlF_6	60.25
2	Cryolithionite	Na_3 ($Li_3Al_2F_{12}$)	10.10
3	Elpasolite	K_2 ($NaAlF_6$)	8.41
4	Fluorite	CaF_2	2.12
5	Aluminium oxide	Al_2O_3	1.49
6	Graphite	C	14.35
7	Polydymite	Ni_3S_4	0.18
8	Pyrite	FeS_2	0.22
9	Sphalerite	ZnS	Very few
10	Magnetite	Fe_3O_4	0.43
11	Barite	$BaSO_4$	Very few
12	Pentlandite	$(Fe,Ni)(Fe,Ni)_8S_8$	0.14
13	Magnesium aluminate	$MgAl_2O_4$	2.28
14	Apatite	$Ca_5[PO_4]_3(F,OH)$	0.03
Total	—	—	100.00

Chemical Multielement Analysis of Anode Carbon Residue

Chemical Multielement Analysis

Chemical multi-element analysis was carried out on anode carbon residue, and the analysis results are shown in **Table 1**.

As can be seen from the analysis results in **Table 1**, the content of element F, Al, Na and K in anode carbon residue is 43.27%, 11.77%, 22.44% and 2.77%. The content of C_{total} was 14.16%. Other elements mainly include Ca, S, Fe, Mg and Ni. The loss on ignition is 16.53% at 700°C, 31.00% at 1,000°C, $C_{organic}$ content is 12.28%, and a small amount of Si, etc.

Analysis of Mineral Composition of Anode Carbon Residue

X-Ray Diffraction Analysis

The anode carbon residue was analyzed by X- ray diffractometer. The X-ray diffraction analysis results are shown in **Figure 3**.

The results of X-ray diffraction show that the anode carbon residue is mainly composed of cryolite, cryolithionite, elpasolite, fluorite, graphite, aluminum oxide, magnesium aluminate and so on. Yang et al. (2021) analysis of anode carbon residue found similar composition.

Analysis of the Mineral Liberation Analyzer

Mineral particles in anode carbon residue were analyzed and counted by MLA, scanning electron microscope and X- ray energy spectrometer to determine their mineral composition. The general analysis diagram is shown in **Figure 4**, and the mineral composition and content results are shown in **Table 2**.

X-ray diffraction analysis shows that there are three kinds of cryolite, cryolithionite and elpasolite in anode carbon residue.

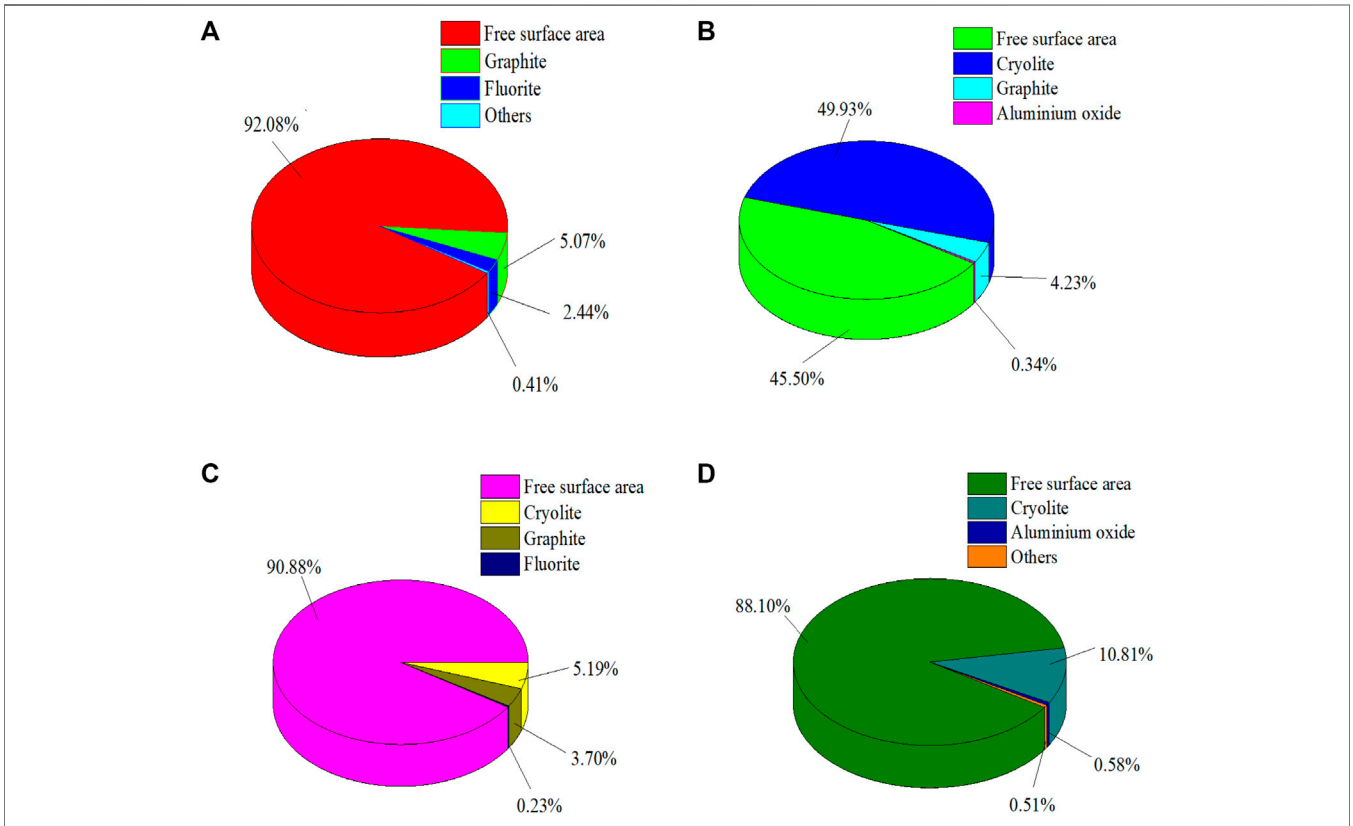

FIGURE 5 | The symbiotic relationships of major minerals. **(A)** The symbiotic relationship between cryolite and other minerals. **(B)** Symbiotic relationship between fluorite and other minerals. **(C)** The symbiotic relationship between aluminum trioxide and other minerals. **(D)** The symbiotic relationship between graphite and other minerals.

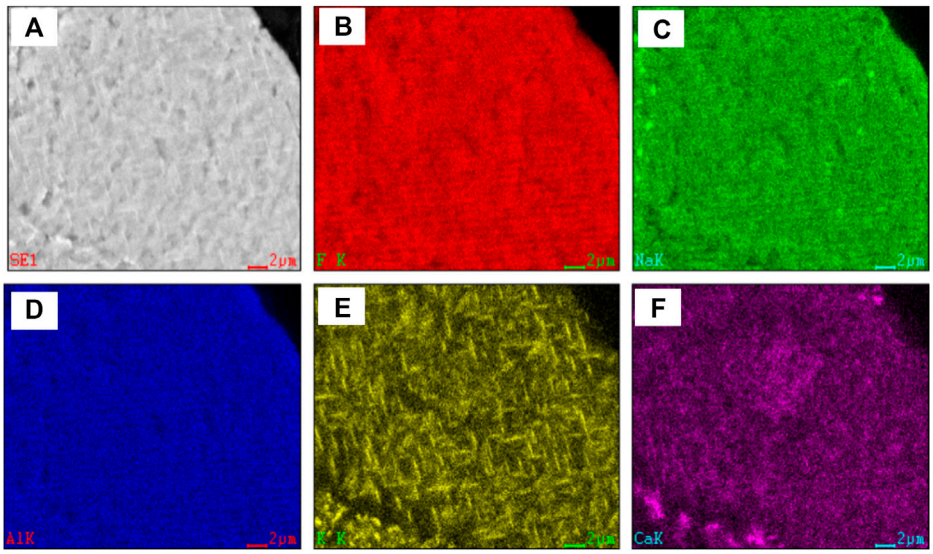

FIGURE 6 | Scanning view of cryolite surface.

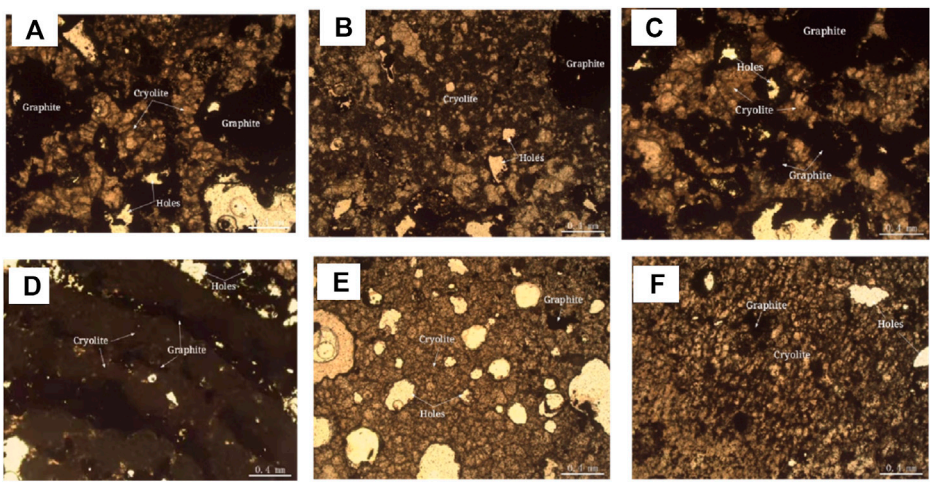

FIGURE 7 | Polarization microscope photo of cryolite (transmitted single polarization). **(A)** Microgranular cryolite, closely inlaid with blurred boundaries and embedded with graphite aggregates. **(B)** The microgranular ice crystals are alternately distributed with micritic cryolite. **(C)** Graphite aggregates are distributed in cryolite. **(D)** The cryolite is in the form of mud-microcrystalline, and the graphite aggregates are in the form of intermittent strips, which are distributed in the cryolite. **(E)** microscopic granular cryolite is shaped granular, particles are closely inlaid, the boundaries are black and thick, and there are more cavities. **(F)** Microgranular cryolite is amorphous and alternately distributed with micritic cryolite.

Because MLA has identification defects for light element lithium, and elpasolite is in fine grid shape and evenly distributed in cryolite and cryolithionite, which is beyond the lower limit of MLA identification, it is difficult to effectively distinguish them. So in MLA analysis, the cryolite, cryolithionite and elpasolite were classified as cryolite for analysis.

According to MLA analysis, combined with X-ray diffraction analysis, rock ore identification analysis and chemical multi-element analysis, the anode carbon residue is composed of 14 minerals, among which cryolite, cryolithionite, elpasolite and graphite are the most important minerals, accounting for about 93%, followed by aluminum oxide, magnesium aluminate and fluorite, accounting for about 6%.

There was only one independent mineral of carbon, graphite, with a content of 14.35%. The independent minerals of fluorine were cryolite, cryolithionite and elpasolite and fluorite, with contents of 60.25%, 10.10%, 8.41%, and 2.12%, respectively. The independent minerals of aluminum are cryolite, cryolithionite

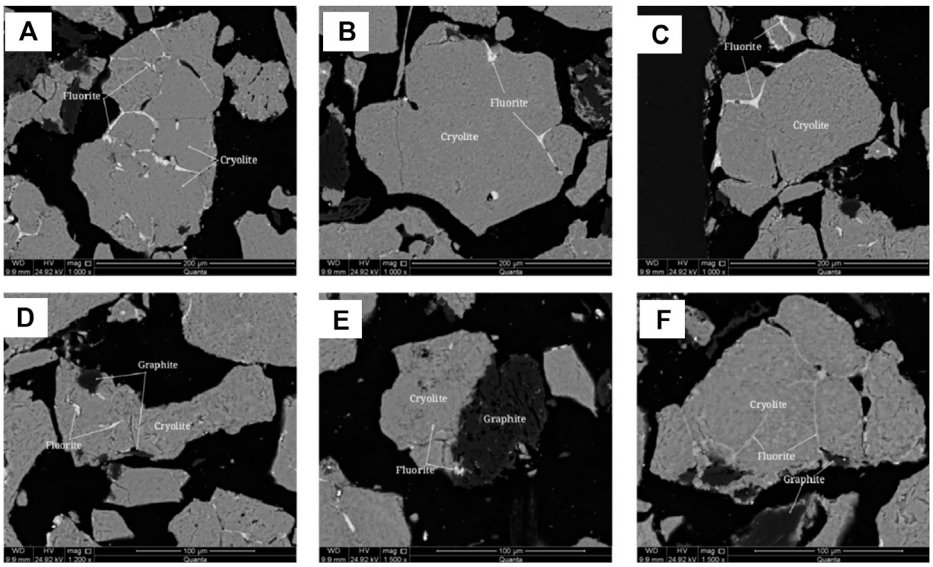

FIGURE 8 | Scanning electron microscope backscattered electron image of cryolite. **(A)** Fluorite filling between cryolite grains; **(B)** Fluorite filling between cryolite grains; **(C)** Fluorite filling between cryolite grains; **(D)** anisotropic granular cryolite particles encapsulate fine fluorite; **(E)** Fine-grained fluorite encapsulated in cryolite; **(F)** Fluorite filling between cryolite grains.

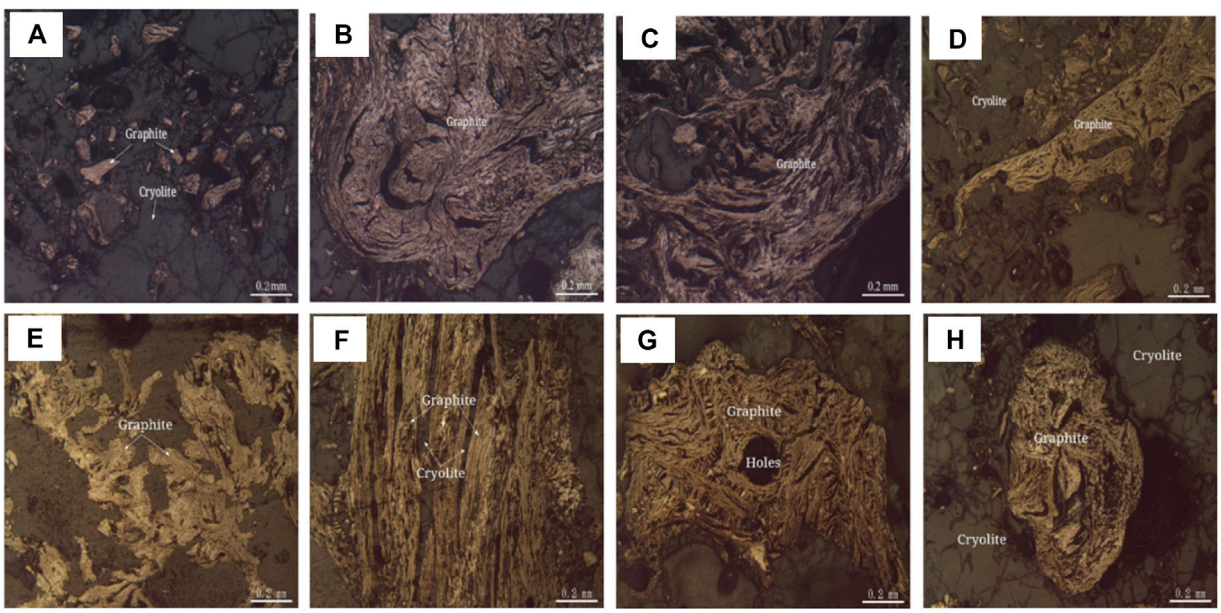

FIGURE 9 | Polarization microscope photo of graphite (Reflected Single Polarized Light). **(A)** Graphite aggregates are amorphous granules distributed between cryolite grains. **(B)** Graphite aggregates are twisted into clumps. **(C)** Fibrous graphite is twisted. **(D)** Graphite aggregates are amorphous granules. **(E)** Flake-like graphite, aggregates are amorphous granular. **(F)** The fibrous graphite aggregates are bundled with cryolite filling between the bundled aggregates. **(G)** Graphite is twisted to be lumpy and camboidal polygonal. **(H)** Graphite aggregates are spherical.

and elpasolite, aluminum oxide and magnesium aluminate, with contents of 60.25%, 10.10%, 8.41%, 1.49%, and 2.28%, respectively. The independent minerals of sodium are cryolite, cryolithionite and elpasolite. The independent mineral of potassium is only a kind of elpasolite.

Symbiotic Relationships of Major Minerals

When the grinding fineness of anode carbon residue is −0.075 mm accounting for 49.74%, MLA is used to analyze the anode carbon residue and make statistics on the symbiosis relationship between the main target minerals in anode carbon

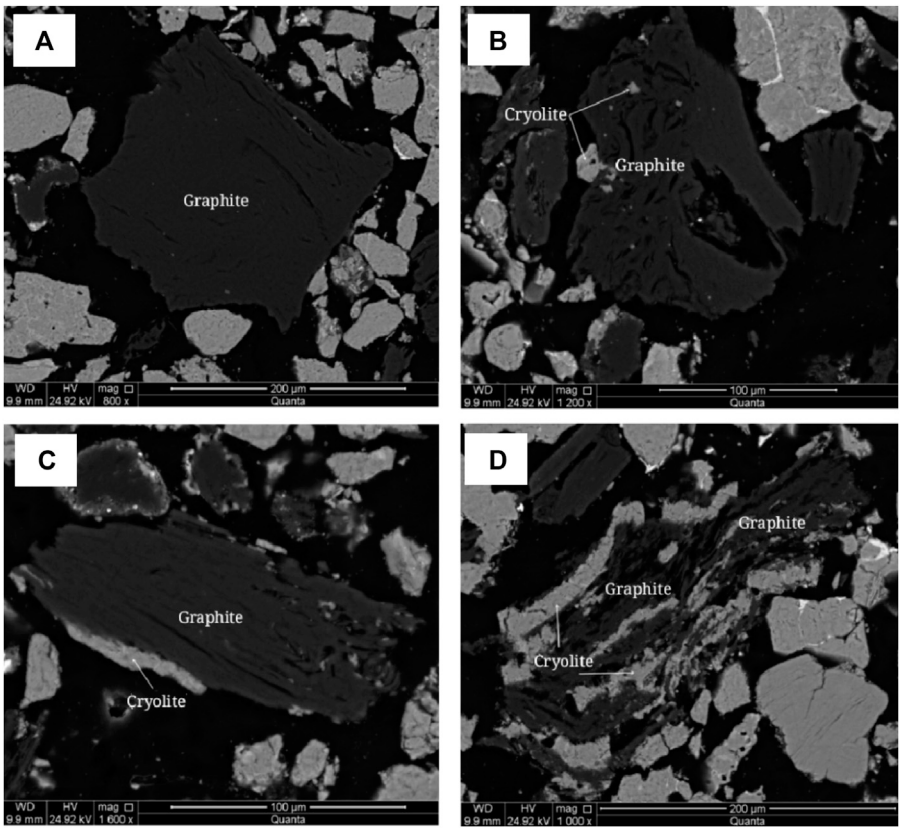

FIGURE 10 | Scanning electron microscope backscattered electron image of graphite. **(A)** Graphite dissociated from monomers. **(B)** Graphite bonded to cryolite or encapsulated with fine grained cryolite. **(C)** Graphite bonded with cryolite. **(D)** Cryolite is distributed in graphite.

residue, cryolite, fluorite, aluminum oxide, graphite and other minerals. The analysis results are shown in **Figure 5**.

The results of **Figure 5** show that the symbiosis relationship of the main minerals in anode carbon residue is relatively simple. Among them, cryolite is mainly associated with graphite fluorite, and the proportion of their common surface area is 5.07% and 2.44%, respectively. The proportion of free surface area of cryolite was 92.08%. Fluorite is mainly associated with cryolite, graphite and aluminum oxide, and the proportions of their common surface area are 49.93%, 4.23% and 0.34%, respectively. The free surface area ratio of fluorite is 45.50%. Aluminum oxide is mainly associated with cryolite, graphite and fluorite, and the proportion of its common surface area is 5.19%, 3.70% and 0.23%, respectively. The free surface area ratio of aluminum oxide was 90.88%. Graphite is mainly associated with cryolite and aluminum oxide, with a total surface area ratio of 10.81% and 0.58%, respectively. The free surface area ratio of fluorite is 88.10%.

Characteristics of Disseminated Particle Size of Carbonaceous Minerals and Fluorine Minerals

Under the condition that the grinding fineness of anode carbon residue is −0.075 mm accounting for 49.74%, the particle size of anode carbon residue and the embedded size characteristic of the main target minerals cryolite, fluorite, aluminum oxide and graphite were analyzed and statistically by using MLA. The analysis results are shown in **Supplementary Figure 1**.

According to the analysis results in **Supplementary Figure 1**, under the current grinding fineness, the cumulative distribution rate of anode carbon residue with +150 μm size is 16.50%, the cumulative distribution rate of +75 μm size is 50.26%, the cumulative distribution rate of +38 μm size is 77.38%, and the cumulative distribution rate of +19 μm size is 92.17%.The cumulative distribution rates of cryolite +150, +75, +38 and +19 μm were 18.24%, 51.55%, 78.91% and 93.70%, respectively. The cumulative distribution rate of fluorite +19 μm was 17.10%, and the cumulative distribution rate of +9.6 μm was 48.97%.The cumulative distribution rates of graphite with 150 μm size were 5.59%, +75 μm size was 29.58%, +38 μm size was 55.02%, and +19 μm size was 75.54%.The cumulative distribution rates of aluminum oxide +75, +38 and +19 μm fractions were 31.30%, 65.53% and 86.92%, respectively.

Mineralogical Characteristics of Major Minerals

The mineralogical characteristics of the main minerals in anode carbon residue were analyzed by polarizing microscope, X-ray

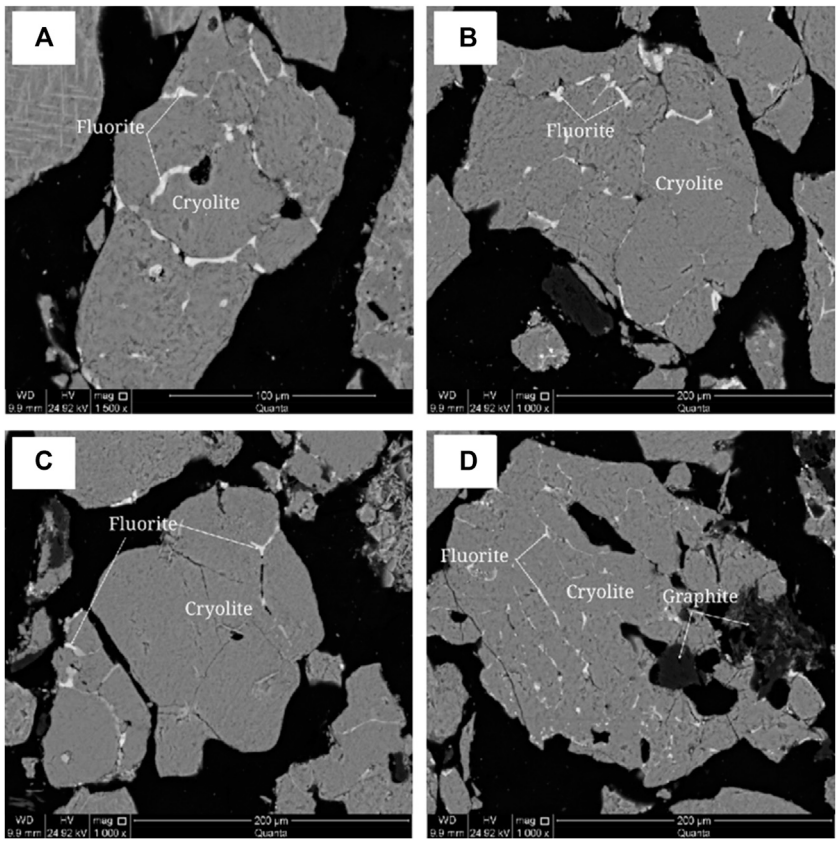

FIGURE 11 | Scanning electron microscope backscattered electron image of fluorite. **(A)** Fluorite aggregates are veined between cryolite grains; **(B)** Fluorite aggregates are veined between cryolite grains; **(C)** Fluorite aggregates are distributed between cryolite grains; **(D)** Fluorite aggregates are veined in cryolite.

energy spectrometer, scanning electron microscope and MLA mineral dissociation analyzer.

Cryolite

The cryolite was analyzed by X-ray energy spectrometer and MLA mineral dispersal analyzer. The X-ray energy spectrum analysis spectrum of cryolite is shown in **Supplementary Figure 2**, and the scanning analysis of mineral surface is shown in **Figure 6**.

As can be seen from **Figure 6**, fluoride, sodium, aluminum and calcium are uniformly distributed without obvious enrichment, while potassium is uniformly distributed, and some of them are grid-like enriched and uniformly distributed.

Polarizing microscope and scanning electron microscope were used to analyze the embedded characteristics of cryolite, as shown in **Figure 7** and **Figure 8**.It is difficult to distinguish cryolite, cryolithionite and elpasolite, so they are classified as cryolite to describe the embedded characteristics under the microscope. Crystalline particle size of cryolite is relatively uniform, most of them are microcrystalline, and the crystal particle size is about 0.1 mm, and it is semi-idiomorphic and anisotomorphic granular. A few cryolite has fine crystal particle size, which is micrite or microcrystalline, and the crystal particle size is < 0.004 mm, or between 0.004 and 0.03 mm. The cryolite particles are closely inlaid, and the boundaries are blurred. The particles are filled with fine fluorite, and some of them are filled with micrite cryolite. The cryolite aggregates have many holes, flake and fibrous flake graphite aggregates are twisted into lumps, camboidal polygonal and other amorphous granules embedded in cryolite.

Graphite

Graphite was analyzed by X-ray energy spectrometer. The X-ray energy spectrum analysis of graphite is shown in **Supplementary Figure 3**. Graphite contained C 98.65% and S 1.35%.

The embedded characteristics of graphite were analyzed by polarizing microscope and scanning electron microscope, as shown in **Figure 9** and **Figure 10**. Graphite crystallization degree is higher, the grain size is larger, flake, fibrous flake, aggregate distortion is lumpy, camboidal polygonal, sharp edges and angles, bundles and other shaped granular. Graphite aggregates are disseminated between 0.05–0.5 and 1.00–2.0 mm, and a few aggregates are disseminated between 2.00 and 3.0 mm and the maximum is 4.0 mm. Graphite aggregates are disseminated between cryolite particles.

Fluorite

The fluorite was analyzed by X-ray energy spectrometer, and the X-ray energy spectrum of fluorite is shown in **Supplementary Figure 4**.

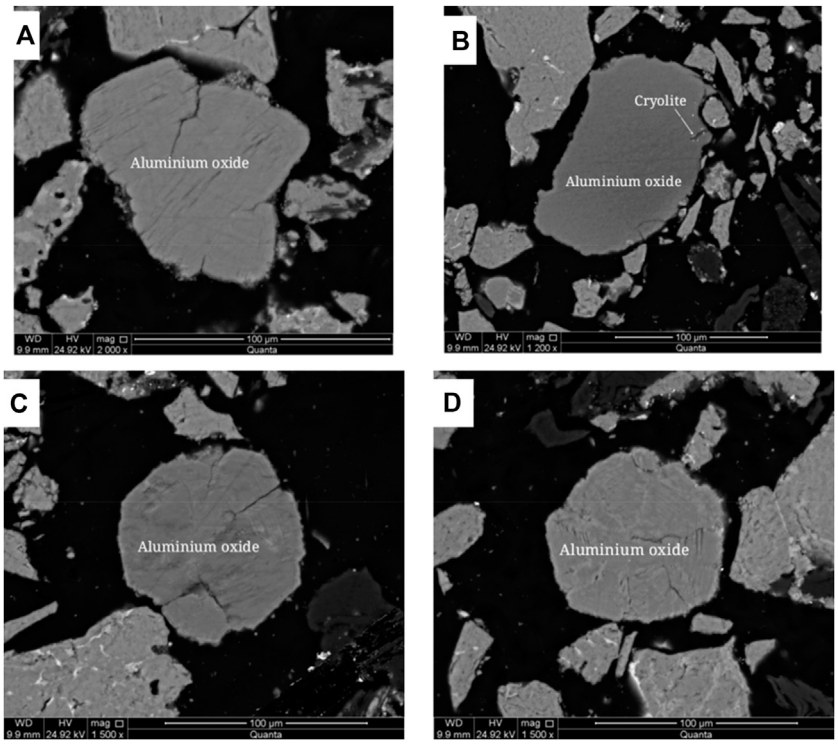

FIGURE 12 | Scanning electron microscope backscattered electron image of aluminum oxide. **(A)** Monomer dissociated aluminum oxide; **(B)** Aluminum oxide is associated with cryolite; **(C)** Monomer dissociated aluminum oxide; **(D)** Monomer dissociated aluminum oxide.

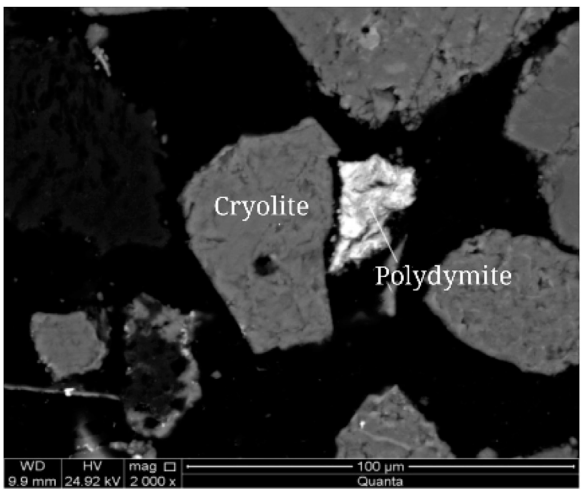

FIGURE 13 | Scanning electron microscope backscattered electron image of Polydymite (Polydymite as crushed granular).

The embedded characteristics of fluorite were analyzed by scanning electron microscopy (SEM), as shown in **Figure 11**. Fluorite is other-shaped granular with fine particle size. The aggregates are mainly other-shaped granular and vein-like distributed among cryolite grains, and a few are granular-coated in cryolite grains and graphite aggregates with disseminated particle size <0.04 mm.

Aluminum Oxide

The X-ray energy spectrometer was used to analyze aluminum oxide. The X-ray energy spectrum analysis of aluminum oxide is shown in **Supplementary Figure 5**.

The embedded characteristics of aluminum oxide were analyzed by scanning electron microscopy (SEM), as shown in **Figure 12**. Aluminum oxide is spherical, mainly associated with cryolite, graphite, and a small amount of fluorite, and the disseminated particle size is < 0.1 mm.

Polydymite

The results of X- ray energy spectrum analysis show that Ni57.86% and S42.14% are in Polydymite. The X-ray energy spectrum analysis spectrum of Polydymite is shown in **Supplementary Figure 6**.

Scanning electron microscopy (SEM) was used to analyze the embedded characteristics of Polydymite, as shown in **Figure 13**. The Polydymite is amorphous and stellate embedded in cryolite, with disseminated particle size < 0.04 mm.

Pyrite

By X-ray energy spectrum analysis, pyrite contains Fe 46.55% and S53.45%. The X-ray energy spectrum analysis spectrum of pyrite is shown in **Supplementary Figure 7**.

The embedded characteristics of pyrite were analyzed by polarizing microscope and scanning electron microscope, as shown in **Figure 14**. Pyrite is amorphous and stellate

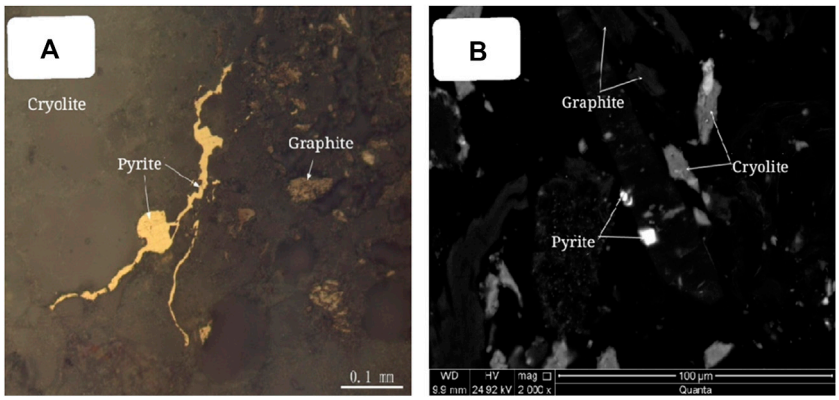

FIGURE 14 | Embedded characteristics of pyrite. **(A)** Pyrite is anamorphic granular (plane polarized light); **(B)** anamorphic granular pyrite (Scanning electron microscope image of backscattered electron).

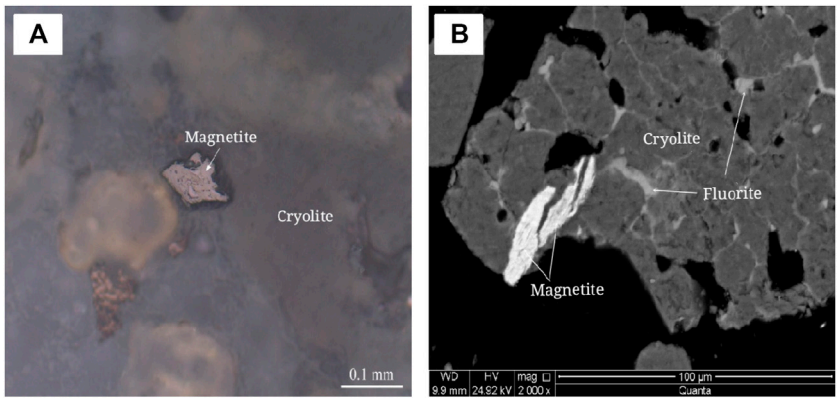

FIGURE 15 | Embedded characteristics of magnetite. **(A)** Anisotropic granular magnetite. plane polarized light. **(B)** Magnetite is encased in cryolite. Scanning electron microscope image of backscattered electron.

TABLE 3 | Calculation of carbon distribution rate in carbonaceous minerals/%.

The name of the mineral	Mineral content	The allocation of C in the mineral	The distribution rate of C in minerals
Graphite	14.35	14.16	100.00
Others	85.65	—	—
Total	100.00	14.16	100.00

embedded in transparent minerals such as cryolite, with disseminated particle size <0.05 mm.

Magnetite

By X-ray energy spectrum analysis, magnetite contains Fe 72.36% and O 27.64%.The X-ray energy spectrum analysis diagram of magnetite is shown in **Supplementary Figure 8**.

The embedded characteristics of magnetite were analyzed by polarizing microscope and scanning electron microscope, as shown in **Figure 15**. Microscopic observation shows that magnetite is amorphous and stellate embedded in transparent minerals such as cryolite, and the disseminated particle size < 0.04 mm.

Occurrence State of the Destination Element

Occurrence State of Carbon

The carbon grade in anode carbon residue is 14.16%, and the carbon occurs in graphite in the form of independent minerals with a distribution rate of 100%. The calculation table of carbon distribution rate in carbon-bearing minerals is shown in **Table 3**.

Occurrence State of Fluorine

The fluorine grade in anode carbon residue is 43.27%, and fluorine occurs in cryolite, cryolithionite, elpasolite and fluorite as independent minerals, with the distribution rates of 74.16, 14.31, 9.15 and 2.38%, respectively. The calculation table of fluorine distribution rate in fluorine-bearing minerals is shown in **Table 4**.

TABLE 4 | Calculation table of the distribution rate of fluorine in fluorine-containing minerals/%.

The name of the mineral	Mineral content	The allocation of F in a mineral	The distribution rate of F in a mineral
Cryolite	60.25	32.09	74.16
Cryolithionite	10.10	6.19	14.31
Elpasolite	8.41	3.96	9.15
Fluorite	2.12	1.03	2.38
Others	19.12	—	—
Total	100.00	43.27	100.00

TABLE 5 | Calculation table of distribution rate of aluminum in aluminum-containing minerals/%.

The name of the mineral	Mineral content	The allocation of Al in a mineral	The distribution rate of Al in minerals
Cryolite	60.25	7.71	65.51
Cryolithionite	10.10	1.46	12.40
Elpasolite	8.41	0.94	7.99
Aluminium oxide	1.49	0.79	6.71
Magnesium aluminate	2.28	0.87	7.39
Others	17.47	—	—
Total	100.00	11.77	100.00

TABLE 6 | Calculation table of sodium distribution rate in sodium-containing minerals/%.

The name of the mineral	Mineral content	The allocation of Na in a mineral	The distribution rate of Na in minerals
Cryolite	60.25	19.76	88.06
Cryolithionite	10.10	1.88	8.38
Elpasolite	8.41	0.80	3.56
Others	21.24	—	—
Total	100.00	22.44	100.00

Occurrence State of Aluminum

The grade of aluminum in anode carbon residue is 11.77%, and aluminum occurs in cryolite, cryolithionite, elpasolite, aluminum oxide and magnesium aluminate in the form of independent minerals, with the distribution rates of 65.51%, 12.40%, 7.99%, 6.71% and 7.39%. The calculation table of aluminum distribution rate in aluminum-bearing minerals is shown in **Table 5**.

Occurrence State of Sodium

The grade of sodium in anode carbon residue is 22.44%, and sodium occurs in cryolite, cryolithionite and elpasolite as independent minerals, with the distribution rates of 88.06%, 8.38% and 3.56%, respectively. The calculation table of sodium distribution rate in sodium-bearing minerals is shown in **Table 6**.

Occurrence State of Potassium

The potassium content in anode carbon residue is 2.77%, and it occurs in the form of independent mineral in potassium cryolite with a distribution rate of 100.00%. The calculation table of potassium distribution rate in potassium-bearing minerals is shown in **Supplementary Table 1**.

CONCLUSION

By studying the occurrence state of the main elements in the anode carbon residue, the content of the main elements in the anode carbon residue was ascertained, and the mineral composition of the anode carbon residue was determined, among which cryolite, cryolithionite, elpasolite and graphite were the most important minerals. The co-associated relationship of the main minerals and the embedded characteristics of carbon minerals and fluorine minerals were investigated.

In the anode carbon residue, the content of carbon is 14.16%, which occurs in graphite as independent minerals. Fluorine content is 43.27%. It occurs in cryolite, cryolithionite, elpasolite and fluorite as independent minerals, and the distribution rate of the three kinds of cryolite reaches 97.62%. The content of aluminum is 11.77%, and it occurs in the form of independent minerals in cryolite, cryolithionite, elpasolite, aluminum oxide and magnesium aluminate. The sodium content is 22.44%, and it occurs in the form of independent mineral in cryolite, cryolithionite, elpasolite. The potassium content is 2.77%, and it occurs in the form of independent

mineral in elpasolite. In terms of occurrence state, fluorine, aluminum, sodium and potassium minerals are mainly distributed in cryolite, cryolithionite, elpasolite, presenting a relatively concentrated distribution. Therefore, the main elements of anode carbon residue, such as fluorine, aluminum, sodium and potassium, mainly occur in cryolite, while carbon mainly occurs in graphite. Effective separation of graphite and cryolite is an effective way to recover and utilize carbon residue. Flotation method can be used to separate carbon and electrolyte mainly containing cryolite.

DATA AVAILABILITY STATEMENT

The original contributions presented in the study are included in the article/**Supplementary Material**, further inquiries can be directed to the corresponding author.

AUTHOR CONTRIBUTIONS

SM: Data curation and Writing- Original draft preparation. ZQ: Conceptualization and Methodology.

FUNDING

This work was financially supported by Project of 100 leading talents in Guizhou Province (Grant No. (2015) 4012).

SUPPLEMENTARY MATERIAL

The Supplementary Material for this article can be found online at: https://www.frontiersin.org/articles/10.3389/fmats.2021.719563/full#supplementary-material

REFERENCES

Allard, F., Désilets, M., and Blais, A. (2019). Thermal, Chemical and Microstructural Characterization of Anode Crust Formed in Aluminum Electrolysis Cells. *Thermochim. Acta* 671, 89–102. doi:10.1016/j.tca.2018.11.008

Aryanpour, G., Alamdari, H., Azari, K., Ziegler, D., Picard, D., and Fafard, M. (2014). Analysis on the Die Compaction Of Anode Paste Material Used in Aluminum Production Plants. *Powder Tech.* 254, 228–234. doi:10.1016/j.powtec.2014.01.033

Azari, K., Alamdari, H., Aryanpour, G., Picard, D., Fafard, M., and Adams, A. (2013). Mixing Variables for Prebaked Anodes Used in Aluminum Production. *Powder Tech.* 235, 341–348. doi:10.1016/j.powtec.2012.10.043

Azari, K., Alamdari, H., Aryanpour, G., Ziegler, D., Picard, D., and Fafard, M. (2013). Compaction Properties of Carbon Materials Used for Prebaked Anodes in Aluminum Production Plants. *Powder Tech.* 246, 650–657. doi:10.1016/j.powtec.2013.06.025

Batista, J. d. S., and Silveira, B. I. d. (2008). Influence of the Sodium Content on the Reactivity of Carbon Anodes. *Mat. Res.* 11, 387–390. doi:10.1590/S1516-14392008000300025

Bhattacharyay, D., Kocaefe, D., Kocaefe, Y., and Morais, B. (2017). An Artificial Neural Network Model for Predicting the CO2 Reactivity of Carbon Anodes Used in the Primary Aluminum Production. *Neural Comput. Applic* 28, 553–563. doi:10.1007/s00521-015-2093-7

Chevarin, F., Lemieux, L., Picard, D., Ziegler, D., Fafard, M., and Alamdari, H. (2015). Characterization of Carbon Anode Constituents under CO 2 Gasification: A Try to Understand the Dusting Phenomenon. *Fuel* 156, 198–210. doi:10.1016/j.fuel.2015.04.035

Dan-qing, Z. (2008). The Measures to Reduce the Consumption of Anode Carbon in Aluminum Electrolysis. *Light Met.* 08, 25–28.

Diógenes, L., Maia, R., Bessa, I., Castelo Branco, V., Nogueira Neto, J., and Silva, F. (2021). The Influence of Crushing Processes and Mineralogy of Aggregates on Their Shape Properties and Susceptibility to Degradation. *Construction Building Mater.* 284, 122745. doi:10.1016/j.conbuildmat.2021.122745

Einarsrud, K. E. (2010). The Effect of Detaching Bubbles on Aluminum-Cryolite Interfaces: An Experimental and Numerical Investigation. *Metall. Materi Trans. B* 41, 560–573. doi:10.1007/s11663-010-9345-9

Grjotheim, K., and Krohn, M. (2020). *Aluminium Electrolysis: Fundamentals of the Hall-Heroult Process*. Dusseldorf, Germany: Aluminium Verlag Marketing & Kommunikation GmbH.

Guo, Y., Yu, Y., Ren, H., and Xu, L. (2020). Scenario-based DEA Assessment of Energy-Saving Technological Combinations in Aluminum Industry. *J. Clean. Prod.* 260, 121010. doi:10.1016/j.jclepro.2020.121010

Hai-fei, X., Li-jun, F., Yang, Z., He-kui, L., and Yi, S. (2009). Analysis of Sources of Carbon Residue and its Control Methods. *Carbon Tech.* 28, 41–44. doi:10.3969/j.issn.1001-3741.2009.06.009

Haupin, W. E. (1971). A Scanning Reference Electrode for Voltage Contours in Aluminum Smelting Cells. *Jom* 23, 46–49. doi:10.1007/BF03355737

Huang, Y., Wang, Z., Yang, Y., Gao, B., Shi, Z., and Hu, X. (2018). Anodic Bubble Behavior in a Laboratory Scale Transparent Electrolytic Cell for Aluminum Electrolysis. *Metals* 8, 806. doi:10.3390/met8100806

Hussein, A., Lu, Y., Mollaabbasi, R., Tessier, J., and Alamdari, H. (2020). Bio-pitch as a Binder in Carbon Anodes for Aluminum Production: Bio-Pitch Properties and its Interaction with Coke Particles. *Fuel* 275, 117875. doi:10.1016/j.fuel.2020.117875

Jin-sheng, L., and Qing-chun, W. (2017). XRD Measurment of Carbon Concentration of Anode Slag in Aluminum Electrolyte. *Phys. Examination Test.* 35, 27–30.

Jing, Y., Xian-lei, L., Du, Bin-bin., Ping-fu, W., and Lu-ning, J. (2010). The Impact of Element in Pre-baked Carbon Anodes on Aluminum Electrolysis and Relevant Control Measures. *Carbon* 144, 37–41. doi:10.3969/j.issn1001-8948.2010.04-008

Jing-lu, W., Zhong-yu, Q., Jun, L., Li, L., and Xian-yong, M. (2015). The Analysis and Control of Fe Content Influencing Factor in Electrolytic Liquid Aluminum. *Yunnan Metall.* 44, 82–85. doi:10.3969/j.issn.1006-0308.2015.05.019

Khaji, K., and Al Qassemi, M. (2016). The Role of Anode Manufacturing Processes in Net Carbon Consumption. *Metals* 6, 128. doi:10.3390/met6060128

Kubiňáková, E., Danielik, V., and Híveš, J. (2018). Electrochemical Characterization of Multicomponent Sodium Cryolite Electrolytes with High Content of Aluminium Fluoride. *Electrochimica Acta* 265, 474–479. doi:10.1016/j.electacta.2018.01.174

Lifeng, M., Shiliang, L., and Hailiang, Z. (2019). Flotation Process of Recycling Carbon Slag from Electrolytic Aluminium. *Mod. Mining* 35, 33–34. doi:10.3969/j.issn.1674-6082.2019.11.011

Min-zhang, L., and Xian, L. (2012). The Effect of Exterior Geometric Shape of Prebaked Anode on the Formation of Carbon Residue during Eletrolysis. *Carbon Tech.* 31, 64–66.

Qing, L., Xudong, C., and Wenyi, G. (2015). Countermeasures and Origins of Carbon Residue in Aluminum Reduction Production. *Light Met.* 11, 36–38. doi:10.13662/j.cnki.qjs.2015.11.008

Xiangyang, M., Jun, L., and Zhanliang, Y. (2016). The Research on Recycling Carbon Residue by Floatation Process. *Light Met.* 04, 28–30. doi:10.13662/j.cnki.qjs.2016.04.007

Xiao, S.-j., Mokkelbost, T., Paulsen, O., Ratvik, A. P., and Haarberg, G. M. (2014). SnO2-based Gas (Hydrogen) Anodes for Aluminum Electrolysis. *Trans. Nonferrous Met. Soc. China* 24, 3917–3921. doi:10.1016/S1003-6326(14)63551-2

Xugui, Z. (2021). Production Practice of Anode Carbon Block Structure Optimization to Reduce Gross Consumption. *Light Met.* 03, 40–44. doi:10.13662/j.cnki.qjs.2021.03.009

Yang, F., Yu, Q., Zuo, Z., and Hou, L. (2021). Thermodynamic Analysis of Waste Heat Recovery of Aluminum Dross in Electrolytic Aluminum Industry. *Energy*

Sourc. A: Recovery, Utilization, Environ. Effects 43, 1047–1059. doi:10.1080/15567036.2019.1634163

Yao-jian, R., Zhi, S., Jie, T., and Wei, L. (2009). Study on Electrolytic Aluminium Carbon Anode Preparation with Calcined Anthracite. *Proced. Earth Planet. Sci.* 1, 694–700. doi:10.1016/j.proeps.2009.09.109

Zhi-qian, W., Tie-jun, W., and Hong-tao, Z. (2019). Analysis and Research on Resource Utilization Technology of Anode Carbon Slag Disposal in Aluminum Electrolysis Production. *World Nonferrous Met.* 22, 8–9. doi:10.3969/j.issn.1002-5065.2019.22.004

Conflict of Interest: The authors declare that the research was conducted in the absence of any commercial or financial relationships that could be construed as a potential conflict of interest.

Publisher's Note: All claims expressed in this article are solely those of the authors and do not necessarily represent those of their affiliated organizations, or those of the publisher, the editors and the reviewers. Any product that may be evaluated in this article, or claim that may be made by its manufacturer, is not guaranteed or endorsed by the publisher.